Inorganic Chemistry

pubs.acs.org/IC Article

Homo/Heteropentanuclear Porphyrazine Mg^{II}, Zn^{II}, and Pd^{II} Macrocycles with Externally Pending $PdCl_2$ and $Pd(CBT)_2$ Units: Synthesis, Physicochemical Characterization, and Photoactivity Studies

Noemi Bellucci, Maria Pia Donzello,* Elisa Viola, and Claudio Ercolani

Cite This: https://doi.org/10.1021/acs.inorgchem.1c01195 Read Online

ACCESS | Metrics & More | Article Recommendations

ABSTRACT: Recent work has been developed on two new classes of neutral porphyrazine complexes of formulas $[(PdCl_2)_4Py_8PzM]\cdot xH_2O$ (Py_8Pz = octakis(2-pyridyl)porphyrazinato anion; M = $Mg^{II}(H_2O)$, Zn^{II}, Pd^{II}) and $[\{Pd(CBT)_2\}_4Py_8PzM]\cdot xH_2O$ (M = $Mg^{II}(H_2O)$, Zn^{II}; CBT = *m*-carborane-1-thiolate anion). Characterization of all of the species has been conducted by IR and UV–visible spectral measurements in a systematic comparison with the related already known mononuclear species $[Py_8PzM]$ (M = $Mg^{II}(H_2O)$, Zn^{II}) and the Pd^{II} analogue isolated and presented for the first time. Systematic comparison includes also the two parent classes of pentanuclear tetrapyrazinoporphyrazines having the more extended π-electron delocalized macrocyclic core $Py_8TPyzPz$. The reported new classes of pentanuclear complexes behave as active photosensitizers in photodynamic therapy (PDT), and due to the high boron content of the CBT derivatives, perspectives for them are open of application in the field of bimodal PDT/boron neutron capture therapy (BNCT) anticancer treatments.

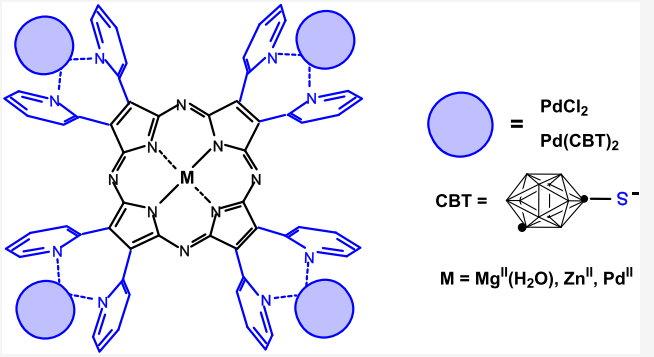

INTRODUCTION

The extended research work conducted by our group on the synthetic and structural aspects and general physicochemical properties of the class of macrocyclic tetrapyrazinoporphyrazines,[1] primarily regarding mononuclear metal derivatives of formula $[Py_8TPyzPzM]\cdot xH_2O$[2] ($Py_8TPyzPz$ = tetrakis-2,3-[5,6-di(2-pyridyl)pyrazino]porphyrazinato anion; M = bivalent metal ion; Figure 1), allowed isolation of several new types of macrocycles. The different studied series included homo/heteropentametallic,[2c,d,3] homo/heterobinuclear neutral and related hexacationic macrocycles,[4] water-soluble,[5a] and mononuclear octacationic and dinuclear heterobimetallic hexacationic water-soluble complexes,[2b,5b] most of them studied as potential photosensitizers for the generation of singlet oxygen, $^1O_2$, the cytotoxic agent in the anticancer treatment known as photodynamic therapy (PDT)[2c,d,3] or in parallel fields of biochemical interest.[6]

Recent work allowed also to further report on the already known neutral pentanuclear pyrazinoporphyrazine complexes $[(PdCl_2)_4Py_8TPyzPzM]\cdot xH_2O$[2c,d,3] and the parallel series of analogues carrying externally *m*-carborane-1-thiolate groups (CBT) of formula $[\{Pd(CBT)_2\}_4Py_8TPyzPzM]\cdot xH_2O$ (M = $Mg^{II}(H_2O)$, Zn^{II}, Pd^{II}).[7] These two series of pentanuclear species behave as active photosensitizers in PDT, and perspectives are also open for the use of the CBT derivatives, due to their high boron content, in the area of boron neutron capture therapy (BNCT). Based on these results, a step forward has been made in the present work with the synthesis of the two related series of macrocyclic complexes, i.e., $[(PdCl_2)_4Py_8PzM]\cdot xH_2O$ (Figure 2A; M = $Mg^{II}(H_2O)$, Zn^{II}, Pd^{II}) and $[\{Pd(CBT)_2\}_4Py_8PzM]\cdot xH_2O$ (Py_8Pz = octakis(2-pyridyl)porphyrazinato anion) (M = $Mg^{II}(H_2O)$, Zn^{II}; Figure 2B). The common feature of these new macrocycles is that all of them are characterized by a more restricted π-electron delocalized Py_8Pz central core with respect to that present in the parallel series of $Py_8TPyzPz$ complexes (Figure 1), this prefigurating different physicochemical properties, among them higher solubility in nonaqueous solvents favored cellular access (pertinent in the case of biochemical studies), a comparable level of expected photoactivity in PDT. In addition, for the CBT derivatives, further results are expected

Received: April 19, 2021

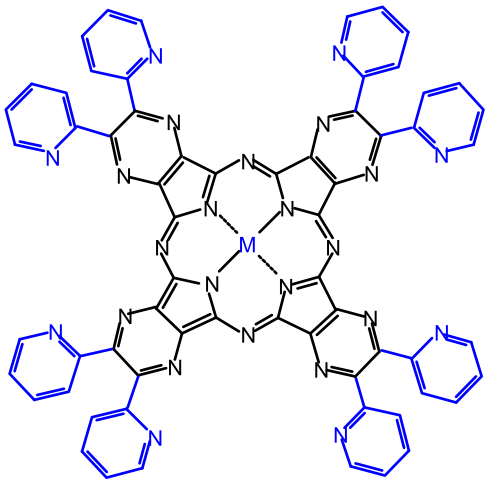

Figure 1. Schematic representation of the pyrazinoporphyrazine macrocycle [$Py_8TPyzPzM$] (M = bivalent metal ion; water molecules neglected).

in the anticancer boron neutron capture therapy (BNCT), this announcing presumable potential applications in the bimodal anticancer modality PDT/BNCT.

EXPERIMENTAL SECTION

Solvents were purchased from Sigma-Aldrich and used as received unless differently specified as follows: pyridine was dried by refluxing over CaO; dimethylformamide (DMF, RPE C. Erba) was used as purchased; and dimethyl sulfoxide (DMSO, RPE C. Erba) was freshly distilled over CaH_2. *m*-Carborane-1-thiol ($HSC_2B_{10}H_{11}$, CBTH) was purchased from Katchem Ltd. and used as received. $[(C_6H_5CN)_2PdCl_2]$[8] and the porphyrazine macrocycles [Py_8PzM]·xH_2O (M = $Mg^{II}(H_2O)$,[9] Zn^{II}[10]) were prepared according to previously reported procedures.

[$(PdCl_2)_4Py_8PzMg(H_2O)$]·H_2O. The complex [$Py_8PzMg(H_2O)$]·$4H_2O$ (12.5 mg, 0.012 mmol) and $(C_6H_5CN)_2PdCl_2$ (24.7 mg, 0.064 mmol) were added to a small flask (10 mL) containing $CHCl_3$ (2 mL), and the mixture was kept under stirring at room temperature for 5 h. The bright green solid was separated by centrifugation, washed twice with $CHCl_3$ and brought to constant weight under vacuum (10^{-2} mmHg; 10.0 mg, yield 49%). Calcd. for [$(PdCl_2)_4Py_8PzMg(H_2O)$]·H_2O, $C_{56}H_{36}Cl_8MgN_{16}O_2Pd_4$: C, 39.58; H, 2.14; N, 13.19; Pd, 25.06%. Found: C, 39.80; H, 2.94; N, 12.88; Pd, 25.88%. IR (cm^{-1}): 2197 (vw), 1598 (m), 1550 (w-m), 1464 (m-s), 1414 (w), 1366 (vw), 1284 (w), 1240 (w), 1218 (vw), 1151 (m), 1105 (w), 1059 (vw), 1031 (w-m), 989 (vs), 877 (w), 828 (w), 774 (s), 755 (w), 722 (w), 651 (vw), 613 (w), 546 (vw), 529 (vw), 328 (m; $\nu_{(Pd-Cl)}$). UV−visible spectral data (λ, nm (log ε)) in DMSO: 391 (4.62), 589 (4.08), 651 (4.74), 723 (3.96); in DMF: 389 (4.60), 588 (4.15), 646 (4.63), 725 (4.2).

[$(PdCl_2)_4Py_8PzZn$]·$22H_2O$. The complex [Py_8PzZn]·$12H_2O$ (20.0 mg, 0.0165 mmol), prepared from the previously reported Mg^{II} analogue via a transmetalation process $Mg^{II} \rightarrow Zn^{II}$,[10] and $(C_6H_5CN)_2PdCl_2$ (31.7 mg, 0.083 mmol) were added to a small flask (10 mL) containing $CHCl_3$ (2 mL), and the mixture was kept under stirring at room temperature for 5 h. The bright green solid was separated by centrifugation, washed twice with $CHCl_3$, and brought to constant weight under vacuum (10^{-2} mmHg; 28.0 mg, yield 81%). Calcd. for [$(PdCl_2)_4Py_8PzZn$]·$22H_2O$, $C_{56}H_{76}Cl_8N_{16}O_{22}Pd_4Zn$: C, 32.03; H, 3.65; N, 10.67; Pd, 20.27%. Found: C, 31.99; H, 3.44; N, 10.19; Pd, 20.88%. IR (cm^{-1}): 2190 (vw), 1592 (m), 1552 (w), 1462 (m), 1416 (vw), 1362 (vw), 1282 (vw), 1238 (vw), 1149 (w-m), 1103 (vw), 1031 (w), 989 (s), 875 (w), 830 (w), 774 (w-m), 751 (vvw), 718 (w), 607 (w), 575 (vvw), 529 (vvw), 462 (vvw), 446 (vvw), 423 (vvw), 395 (vvw), 366 (vvw), 349 (vw)/337 (vw) (split $\nu_{(Pd-Cl)}$). UV−visible spectral data (λ, nm (log ε)) in DMSO/HCl 0.2 mM: 391 (4.54), 588 (4.04), 645 (4.60); in DMF/HCl 0.2 mM: 396 (4.49), 587 (4.02), 643 (4.66).

[$(PdCl_2)_4Py_8PzPd$]·$10H_2O$. Given the occurrence of a transmetalation process of the type $Mg^{II} \rightarrow Pd^{II}$ (effectively occurring) is possible, the synthesis of this homopentanuclear complex was performed starting from the related mononuclear Mg^{II} complex [$Py_8PzMg(H_2O)$]·$4H_2O$ by reaction with $PdCl_2$ in DMSO: [$Py_8PzMg(H_2O)$]·$4H_2O$ (20.8 mg, 0.0214 mmol) was suspended (partially dissolved) in DMSO (1.5 mL). After addition of $PdCl_2$ (26.6 mg, 0.150 mmol), the mixture was heated at 120 °C for 6 h. After cooling, the solid material was separated by centrifugation, washed with water and acetone, and brought to constant weight under vacuum (10^{-2} mmHg; 12.8 mg, yield 34%). Calcd. for [$(PdCl_2)_4Py_8PzPd$]·$10H_2O$, $C_{56}H_{52}Cl_8N_{16}O_{10}Pd_5$: C, 34.94; H, 2.72; N, 11.64; Pd, 27.64%. Found: C, 35.04; H, 2.70; N, 10.68; Pd, 28.10%. IR (cm^{-1}): 3459 (vs), 3111 (vvw), 3073 (w), 1614 (m-s), 1600 (vvw), 1563 (w), 1494 (vw), 1474 (vs), 1424 (w), 1381 (w), 1292 (w), 1248 (w-m), 1228 (vvw), 1183 (w-m), 1164 (w), 1134 (vvw), 1112 (w), 1091 (vvw), 1065 64 (vvw), 1040 (m), 1013 (s), 985 (w), 899 (w), 861 (vw), 842 (w-m), 830 (vvw), 814 (vvw), 776 (s), 738 (m), 711 (w), 677 (vvw), 653 (vvw), 623 (vw), 604 (w), 557 (w), 533 (w), 326 (vvw; $\nu_{(Pd-Cl)}$). UV−visible spectral data (λ, nm (log ε)) in DMSO/HCl 0.2 mM: 347, 561, 625; in DMF/HCl 0.2 mM: 342, 563, 617. Previous attempts to prepare the same

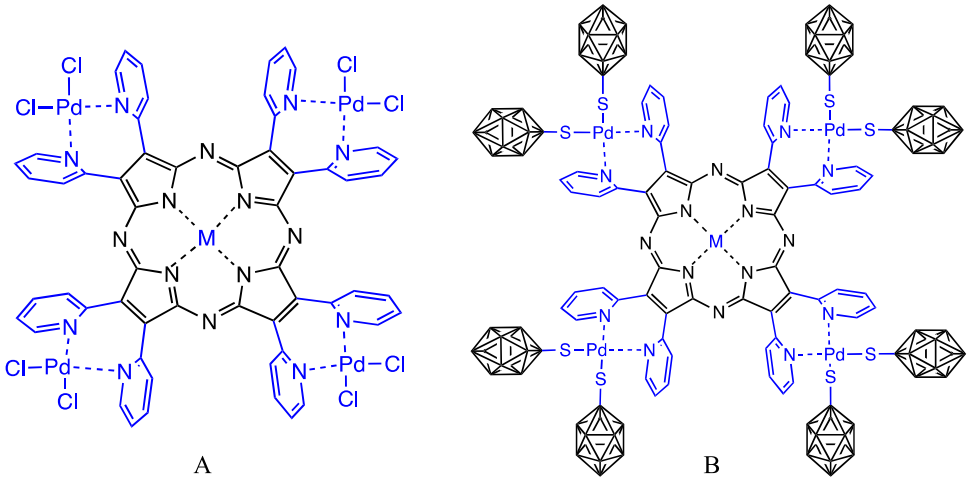

Figure 2. Schematic structure of the complexes [$(PdCl_2)_4Py_8PzM$] (M = $Mg^{II}(H_2O)$, Zn^{II}, Pd^{II}) (A) and [$\{Pd(CBT)_2\}_4Py_8PzM$] (M = $Mg^{II}(H_2O)$, Zn^{II}) (B) (water molecules neglected).

https://doi.org/10.1021/acs.inorgchem.1c01195
Inorg. Chem. XXXX, XXX, XXX−XXX

homopentanuclear species under different experimental conditions ($(C_6H_5CN)_2PdCl_2$ in $CHCl_3$) were unsuccessful, leading probably to the tetrapalladated unmetalated species $[(PdCl_2)_4Py_8PzH_2]$; formulation of this latter appears to be confirmed by the fact that its reaction with $M(OAc)_2$ (M = Mg^{II} and Zn^{II}) leads to the formation of the corresponding tetrapalladated metal complexes $[(PdCl_2)_4Py_8PzM]$ (M = $Mg^{II}(H_2O)$, Zn^{II}) above reported.

$[Py_8PzPd]\cdot 4H_2O$. This complex was obtained upon detachment of exocyclic $PdCl_2$ units from the related pentanuclear species $[(PdCl_2)_4Py_8PzPd]\cdot 10H_2O$ as follows: $[(PdCl_2)_4Py_8PzPd]\cdot 10H_2O$ (9.0 mg, 5.16×10^{-3} mmol) was suspended in a 3% NH_3 aqueous solution (1 mL), and the mixture was stirred for 2 h at room temperature. After centrifugation, the solid material was washed with water to neutrality and then with acetone and brought to constant weight under vacuum (10^{-2} mmHg; 3.5 mg, yield 61%). Calcd. for $[Py_8PzPd]\cdot 4H_2O$, $C_{56}H_{40}N_{16}O_4Pd$: C, 60.73; H, 3.64; N, 20.24; Pd, 9.61. Found: C, 61.55; H, 3.47; N, 19.63; Pd, 10.05%. IR (cm^{-1}): 3439 (vs), 3051 (vw), 2920 (vw), 1632 (w), 1584 (vw), 1563 (w), 1490 (vvw), 1463 (w-m), 1421 (w-m), 1384 (vvw), 1370 (w), 1284 (vw), 1240 (vw), 1176 (w), 1151 (w), 1117 (vw), 1093 (w), 1051 (w), 1018 (m), 998 (vvw), 976 (vvw), 896 (w), 860 (w), 842 (w), 830 (vvw), 814 (vvw), 799 (vvw), 773 (vw), 752 (vvw), 738 (w), 709 (w), 676 (vvw), 606 (vvw), 599 (vw), 579 (vvw), 554 (w), 528 (vw), 500 (vvw). UV−visible spectral data (λ, nm (log ε)) in DMSO/HCl 0.2 mM: 339 (4.42), 562 (3.95), 617 (4.44); in DMF/HCl 0.2 mM: 339 (4.73), 426 (4.24), 557 (4.35), 612 (4.87), 659 (4.40); in py: 341 (4.55), 563 (4.19), 617 (4.74).

$[\{Pd(CBT)_2\}_4Py_8PzMg(H_2O)]\cdot 30H_2O$. $[(PdCl_2)_4Py_8PzMg(H_2O)]\cdot H_2O$ (5.2 mg, 3.06×10^{-3} mmol) and *m*-carborane-1-thiol (7.55 mg, 0.043 mmol) were introduced into a flask (10 mL) containing 2 mL of CH_3CN, and the mixture was refluxed at 90 °C for 4 h. After cooling, the brown solution was centrifuged and a dark green solid was separated from the mother liquor. The solid was washed with CH_3CN and brought to constant weight under vacuum (10^{-2} mmHg; 6.0 mg, 59%). Calcd. for $[\{Pd(CBT)_2\}_4Py_8PzMg(H_2O)]\cdot 30H_2O$, $C_{72}H_{182}B_{80}MgN_{16}O_{31}Pd_4S_8$: C, 25.89; H, 5.49; N, 6.71; S, 7.68; Pd, 12.75%. Found: C, 25.02; H, 4.58; N, 6.52; S, 8.37; Pd, 12.86%. IR (cm^{-1}): 3061 (vvw), 2602 (s), 1632 (w), 1560 (vw), 1468 (w), 1423 (vvw), 1288 (vw), 1244 (vvw), 1161 (w), 1134 (vvw), 1076 (w-m), 1034 (vw), 1003 (vw), 980 (vw), 858 (w), 827 (vw), 779 (w-m), 727 (m), 708 (vw), 669 (w-m), 656 (vw), 617 (vvw), 602 (vvw), 526 (vvw), 430 (vvw). UV−visible spectral data (λ, nm (log ε)) in DMSO: 378 (4.59), 452 (4.38), 579 (4.19), 637 (4.53), 733 (3.89); in DMF: 378 (4.87), 447 (4.59), 582 (4.34), 635 (4.84), 724 (3.89).

$[\{Pd(CBT)_2\}_4Py_8PzZn]\cdot 18H_2O$. $[(PdCl_2)_4Py_8PzZn]\cdot 22H_2O$ (14 mg, 6.67×10^{-3} mmol) and m-carborane-1-thiol (16.45 mg, 0.093 mmol) were introduced into a flask (10 mL) containing 5 mL of CH_3CN, and the mixture was refluxed at 90 °C for 4 h. After cooling, the brown solution was centrifuged and a bright green solid was separated from the mother liquor. The product was washed with CH_3CN and brought to constant weight under vacuum (10^{-2} mmHg; 16.1 mg, 76%). Calcd. for $[\{Pd(CBT)_2\}_4Py_8PzZn]\cdot 18H_2O$, $C_{72}H_{156}B_{80}N_{16}O_{18}Pd_4S_8Zn$: C, 27.48; H, 5.00; N, 7.12; S, 8.15; Pd, 13.53%. Found: C, 27.09; H, 4.55; N, 6.85; S, 8.60; Pd, 13.33%. IR (cm^{-1}): 3041 (vw), 2585 (s), 1590 (w), 1552 (vw), 1464 (w), 1418 (vvw), 1360 (vvw), 1284 (vvw), 1238 (vvw), 1149 (w), 1100 (vvw), 1069 (vw), 1023 (vw), 987 (w-m), 877 (vvw), 853 (vvw), 830 (vvw), 778 (w), 722 (w-m), 607 (vw), 320 (vvw). UV−visible spectral data (λ, nm (log ε)) in DMSO: 379 (4.86), 454 (4.44), 579 (4.33), 635 (4.92); in DMF: 379 (4.91), 448 (4.52), 580 (4.33), 635 (4.98).

Singlet Oxygen Quantum Yield Measurements. Measurements of singlet oxygen quantum yield (Φ_Δ) were carried out as previously reported in DMF and/or DMF/HCl ([HCl] = (1−2) × 10^{-4} M) by an absolute method using 1,3-diphenylisobenzofuran (DPBF) as the scavenger of singlet oxygen ($^1O_2$).[11] Solutions of the complexes (ca. 10^{-6}−10^{-5} M) and DPBF (ca. 5×10^{-5} M) in DMF and/or DMF/HCl were irradiated in a 10 mm path length quartz cell with monochromatic light (Premier LC Lasers/HG Lens, Global Laser). The irradiation wavelength (λ_{irr} = 635 or 650 nm) was close to the maximum of the Q-band absorption peaks for each compound. The light intensity was set to 0.300 mW, and the value accurately measured with a radiometer (ILT 1400A/SEL100/F/QNDS2, International Light Technologies). The decay of DPBF absorption at 414 nm ($\varepsilon^{DPBF} = 2.3 \times 10^4$ mol^{-1} L cm^{-1}) was monitored at 20 °C by a Varian Cary 50 Scan UV−visible spectrophotometer. The Φ_Δ values were calculated from the Stern−Volmer plots on the basis of eq 1

$$\frac{1}{\Phi_{DPBF}} = \frac{1}{\Phi_\Delta} + \frac{k_d}{k_r}\frac{1}{\Phi_\Delta}\frac{1}{[DPBF]} \quad (1)$$

where Φ_{DPBF} is the quantum yield of the photoreaction, k_d is the decay rate constant of $^1O_2$ in the solvent, and k_r is the rate constant for the reaction of DPBF with $^1O_2$. The $1/\Phi_\Delta$ values were obtained as the intercept of each linear plot ($1/\Phi_{DPBF}$ versus $1/[DPBF]$).

Other Physical Measurements. IR spectra were recorded on a Varian FT-IR 660 in the range 4000−250 cm^{-1} (KBr pellets or nujol mulls between CsI disks). UV−visible solution spectra were recorded with a Varian Cary 5E spectrometer using 1 cm quartz cuvettes. Elemental analyses for C, H, N, and S were provided by the "Servizio di Microanalisi" at the Dipartimento di Chimica, Università Sapienza (Rome), on an EA 1110 CHNS-O instrument. The ICP PLASMA Pd analyses were performed on a Varian Vista MPX CCD simultaneous ICP-OES. Mass spectra experiments were taken locally with an MS-ESI instrumentation.

RESULTS AND DISCUSSION

Synthesis and General Properties of Homo/Heteropentanuclear Porphyrazines, $[(PdCl_2)_4Py_8PzM]\cdot xH_2O$ (M = $Mg^{II}(H_2O)$, Zn^{II}, Pd^{II}). Following already known reaction procedures for the synthesis of the pyrazinoporphyrazine analogues of formula $[(PdCl_2)_4Py_8TPyzPzM]\cdot xH_2O$ (M = $Mg^{II}(H_2O)$, Zn^{II}),[2c] the present two heteropentanuclear complexes, $[(PdCl_2)_4Py_8PzM]\cdot xH_2O$ (M = $Mg^{II}(H_2O)$, Zn^{II}) (Figure 2A), were obtained (Experimental Section) under mild experimental conditions by reaction of the corresponding previously reported mononuclear species $[Py_8PzM]\cdot xH_2O$[9,10] with $(C_6H_5CN)_2PdCl_2$ in $CHCl_3$. The synthesis of the parent new homopentanuclear Pd^{II} complex $[(PdCl_2)_4Py_8PzPd]\cdot 10H_2O$ (also schematically shown in Figure 2A) was instead made using as reactant the already known Mg^{II} complex $[Py_8PzMg(H_2O)]\cdot 4H_2O$[9] by heating it in DMSO in the presence of an excess of $PdCl_2$, reaction, which implied transmetalation of central Mg^{II} with Pd^{II}. Interestingly, by detachment of exocyclic $PdCl_2$ units from the pentanuclear Pd^{II} complex $[(PdCl_2)_4Py_8PzPd]\cdot 10H_2O$ in NH_3 aqueous solution, the new mononuclear related species $[Py_8PzPd]$ could be isolated. All three new pentanuclear complexes and the parent Pd^{II} mononuclear species were obtained as stable to air bright green amorphous powders An attempt locally conducted of a mass spectral experiment on the just cited pentapalladated species gave a very poor result revealing for the complex the presence of the expected molecular peak having an extremely low intensity, this result not encouraging more experiments on the corresponding Mg^{II} and Zn^{II} macrocycles. In relationship with these findings are also the results of previous MALDI-TOF experiments conducted on the previously reported pyrazinoporphyrazine analogues, which proved the systematic detachment of the external $PdCl_2$ or $Pd(CBT)_2$ with the associated formation of the respective mononuclear macrocycles, as exemplified for: (a) $[(PdCl_2)_4Py_8TPyzPzPd]$,[2c] (b) $[\{Pd(CBT)_2\}_4Py_8TPyzPzM]$ (M = $Mg^{II}(H_2O)$, Zn^{II}, Pd^{II}),[7] and (c) $[\{Pd(CBT)_2\}_4Py_8TPyzPzZn]$.[7] In addition, for the MALDI-TOF spectrum of the complex $[(CN)_2dppPdCl_2]$ (dpp = di(2-

https://doi.org/10.1021/acs.inorgchem.1c01195
Inorg. Chem. XXXX, XXX, XXX−XXX

pyridyl)pyrazine), only a peak of the ligand [$(CN)_2$dpp] was detected.[2c]

The presence of clathrated water molecules is a reproducible common feature for present new species as it is generally for porphyrazine macrocycles carrying externally annulated heterocyclic rings.[2a−d,12,13] The amount of clathrated water, which can change for the different prepared batches of each single species, is generally removed by mild heating (ca. 100 °C) under vacuum (10^{-2} mmHg). Exposure of the heated samples to air leads generally to rehydration of the materials. Due to the limited influence of clathrated water molecules on the general physicochemical properties of the complexes, H_2O will be hereafter neglected in the given formulas (unless required).

The Mg^{II} complex [$(PdCl_2)_4Py_8PzMg(H_2O)$] is formulated with one water molecule axially ligated to Mg^{II} in line with a similar formulation for the related mononuclear derivative [$Py_8PzMg(H_2O)$][9] and also for the parent Py_8TPyzPz complexes [$(PdCl_2)_4Py_8TPyzPzMg(H_2O)$][3] and [$Py_8TPyzPzMg(H_2O)$].[2a] The presence of such a water molecule is difficult to be proved directly, but its presence is encouraged by the fact that the $Mg(H_2O)$ moiety is commonly observed in porphyrazine and phthalocyanine macrocycles carrying Mg^{II} centrally coordinated. As already noticed elsewhere,[2a,7] single-crystal X-ray work has established the presence of axially ligated H_2O to Mg^{II} in the complexes [$(omtp)Mg(H_2O)$][14] (omtp = octakis(methylthio)-porphyrazinato dianion) and [$PcMg(H_2O)$]·2py[15] (Pc = phthalocyaninato dianion, $[C_{32}H_{16}N_8]^{=}$). The presence of H_2O on Mg^{II} was also given some support in the previously reported complexes of the tetrakis(thia/selenodiazole)-porphyrazines.[16] Interestingly, even the complex [$PcMg(H_2O)_2$] bearing two axially ligated water molecules has been reported[17] and a dimerized monohydrate of a Mg^{II} low-symmetry porphyrazine macrocycle has been structurally elucidated.[18]

The quite similar IR spectra of the complexes [$(PdCl_2)_4Py_8PzM$] (M = $Mg^{II}(H_2O)$, Zn^{II}) (data listed in the Experimental Section) are shown in the range 1800−300 cm^{-1} in Figure 3B,C. A noteworthy feature in the spectra is the presence for the Mg^{II} complex of $\nu_{(Pd\text{-}Cl)}$ as a moderately intense absorption located at 328 cm^{-1}, and the same assignment can be proposed for the low-intensity split absorption (349/337 cm^{-1}) observed for the parent Zn^{II} complex, assignments similar to those made for the Py_8TPyzPz analogues [$(PdCl_2)_4Py_8TPyzPzM$] (M = Zn^{II},[3] Pd^{II},[2c] and Cd^{II}[3]). The conversion [Py_8PzM] → [$(PdCl_2)_4Py_8PzM$] (M = $Mg^{II}(H_2O)$, Zn^{II}) determines the disappearance of the intense absorption at 1006 cm^{-1} present for the mononuclear [$Py_8PzMg(H_2O)$] (Figure 3A; a similar absorption for the Zn^{II} analogue occurs at 1005 cm^{-1}),[10] whereas a new low-intensity absorption grows in at 1031 cm^{-1} for both complexes. A second absorption, also typical of the [Py_8PzM] species and located at 983 cm^{-1} for both Mg^{II} and Zn^{II} mononuclear complexes, is still present in the related pentanuclear [$(PdCl_2)_4Py_8PzM$] derivatives and shows only a minimal change of position (989 cm^{-1}) and relevant higher intensity. It is worth noting that these IR spectral features are particularly informative for establishing the complete formation of the pentanuclear species at the end of each synthetic procedure. In the region 900−700 cm^{-1}, the IR spectra of the complexes [$(PdCl_2)_4Py_8PzM$] (M = $Mg^{II}(H_2O)$, Zn^{II}) show a characteristic doublet located at 877/828 cm^{-1} for the Mg^{II} complex

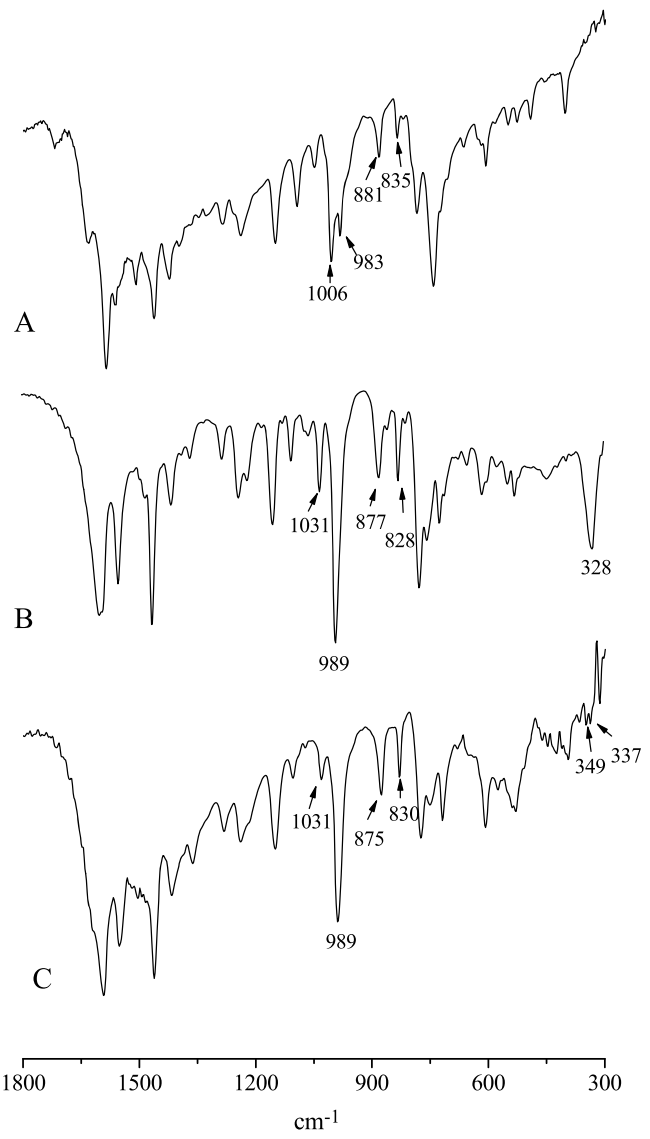

Figure 3. IR spectra in KBr of (A) [$Py_8PzMg(H_2O)$], (B) [$(PdCl_2)_4Py_8PzMg(H_2O)$], and (C) [$(PdCl_2)_4Py_8PzZn$].

and at 875/830 cm^{-1} for the Zn^{II} analogue, thus with position only slightly influenced by the type of central metal ion, which suggests structural similarity for the two metal complexes. Moreover, a similar doublet is also present in the corresponding mononuclear species [Py_8PzM] (M = $Mg^{II}(H_2O)$, Zn^{II}), with a minimally different position (881/835 and 879/833 cm^{-1} for the Mg^{II} and Zn^{II}, respectively),[9,10] this suggesting that the doublet is peculiar of the central macrocyclic framework.

The IR spectra of the mononuclear [Py_8PzPd] and pentanuclear [$(PdCl_2)_4Py_8PzPd$] complexes (not reported) are in line with the findings for the related Mg^{II} and Zn^{II} species, with $\nu_{(Pd\text{-}Cl)}$ located at 326 cm^{-1} for the pentapalladated complex, and absent for the corresponding monomer, as expected.

As illustrated in the schematic representation of Figure 2A, the coordination of the four $PdCl_2$ units in the porphyrazine macrocycles [$(PdCl_2)_4Py_8PzM$] is obviously given as occurring at the N atoms of the pyridine rings ("py−py" coordination), the type of coordination repeatedly observed for the analogues of the more extended pyrazinoporphyrazine macrocycles

https://doi.org/10.1021/acs.inorgchem.1c01195
Inorg. Chem. XXXX, XXX, XXX−XXX

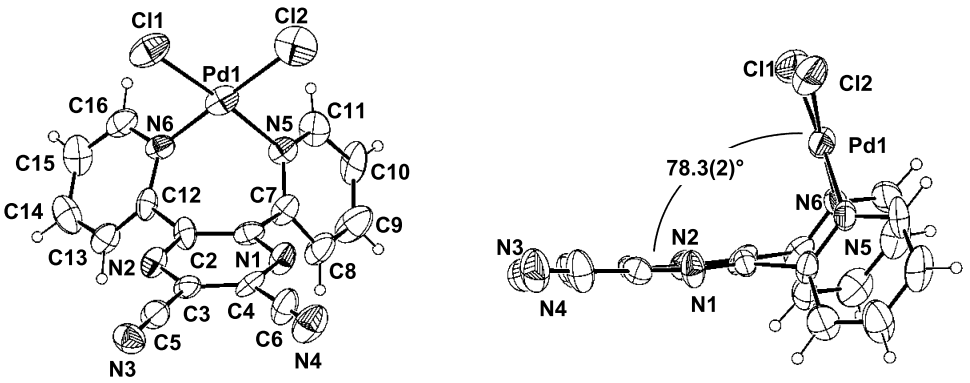

Figure 4. ORTEP front (left) and side (right) views (30% probability ellipsoid) of $[(CN)_2dppPdCl_2]$.[2c]

$[(PdCl_2)_4Py_8TPyzPzM]$ (M = bivalent metal ion)[2c,d,3,13] and unequivocally proved by the X-ray structure of their palladated precursor $[(CN)_2dppPdCl_2]$[2c] (Figure 4), in which the coordination site N_2PdCl_2 is positioned almost perpendicular to the plane of the pyrazine ring.

Synthesis and General Properties of the Heteropentanuclear Porphyrazines Carrying Externally Carborane-1-Thiolate Groups, $[\{Pd(CBT)_2\}_4Py_8PzM]$ (M = $Mg^{II}(H_2O)$, Zn^{II}). As detailed in the Experimental Section, the porphyrazine complexes of formula $[\{Pd(CBT)_2\}_4Py_8PzM]\cdot xH_2O$ (Figure 2B; M = $Mg^{II}(H_2O)$, Zn^{II}) were also obtained as highly hydrated stable-to-air bright green amorphous powders, by reaction of the parent pentanuclear species $[(PdCl_2)_4Py_8PzM]\cdot xH_2O$ with *m*-carborane-1-thiol in CH_3CN (90 °C, 4 h). As for the related pentanuclear $[(PdCl_2)_4Py_8PzM]$ and mononuclear $[Py_8PzM]$ species, hereafter, formulation of the new CBT macrocyclic derivatives will be made neglecting the presence of the water molecules.

The Mg^{II} complex $[\{Pd(CBT)_2\}_4Py_8PzMg(H_2O)]$ is formulated with a single H_2O molecule axially coordinated to the metal center, in line with the above-given formulations for Mg^{II} mono- and pentanuclear derivatives, i.e., $[Py_8PzMg(H_2O)]$[9] and the present $[(PdCl_2)_4Py_8PzMg(H_2O)]$. The IR spectra of the two complexes $[\{Pd(CBT)_2\}_4Py_8PzM]$ (M = $Mg^{II}(H_2O)$, Zn^{II}) are practically superimposable in the range of 4000−300 cm^{-1}. Figure 5 reports the spectrum of the Zn^{II} complex in the range of 3200−300 cm^{-1}, which shows a narrow low-intensity peak at 3041 cm^{-1} and a very intense peak at 2585 cm^{-1} assigned, respectively, to the C−H and the B−H stretching vibrations of the *m*-carborane cage.[19] These absorptions are also present in the same positions for the Mg^{II} species, this definitely supporting the presence in the complexes of the peripheral CBT groups. One more peak attributable to the CBT units is also present at 727 cm^{-1} for the $Mg^{II}(H_2O)$ complex and at 722 cm^{-1} for the Zn^{II} complex. Using as reference the spectra of the Zn^{II} complexes, it can be seen that full conversion of $[(PdCl_2)_4Py_8PzZn]$ (Figure 3C) to $[\{Pd(CBT)_2\}_4Py_8PzZn]$ is supported by the fact that the stretching $\nu_{(PdCl)}$ present in the spectrum of the first one is completely absent in the spectrum of the parallel CBT derivative (see the inset in Figure 5, range 400−300 cm^{-1}). The peak present at 987 cm^{-1} for the CBT species is observed also for its externally palladated analogue at a slightly different position (989 cm^{-1}; Figure 3C), while a new low-intensity peak is present at 1020 cm^{-1}. The presence of clathrated water in the two complexes is confirmed by a large intense absorption at 3500−3200 cm^{-1} (not shown) and by the presence of absorptions at ca. 1600 cm^{-1}.

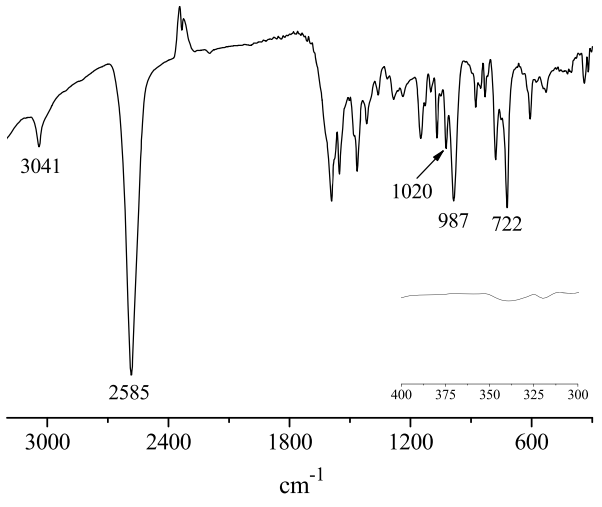

Figure 5. IR spectrum in KBr of $[\{Pd(CBT)_2\}_4Py_8PzZn]$.

UV−Visible Spectral Behavior of the Complexes $[(PdCl_2)_4Py_8PzM]$ (M = $Mg^{II}(H_2O)$, Zn^{II}, Pd^{II}) and $[\{Pd(CBT)_2\}_4Py_8PzM]$ (M = $Mg^{II}(H_2O)$, Zn^{II}). These two series of pentanuclear complexes were sufficiently soluble in DMSO and DMF ($c \sim 10^{-4}$ M), poorly soluble in nondonor solvents ($CHCl_3$, CH_2Cl_2, THF), and completely insoluble in water. Their UV−visible spectral behavior has been examined in solutions of DMSO and DMF (in some cases, in the presence of HCl) in the range 300−900 nm ($c \leq 10^{-5}$ M) outlining the differences between the complexes carrying externally $PdCl_2$ units $[(PdCl_2)_4Py_8PzM]$ (M = $Mg^{II}(H_2O)$, Zn^{II}, Pd^{II}) and their CBT analogues $[\{Pd(CBT)_2\}_4Py_8PzM]$ (M = $Mg^{II}(H_2O)$, Zn^{II}). Appropriate attention has been also given to the spectral features of the related mononuclear macrocycles $[Py_8PzM]$ and of the corresponding series of pyrazinoporphyrazine metal derivatives having the more expanded $Py_8TPyzPz$ central core (ref7 and references therein). For the pentanuclear Zn^{II} complex $[(PdCl_2)_4Py_8PzZn]$, quantitative spectral data were taken in DMSO and DMF in the presence of HCl, from one side addition of the acid leaving unmodified the original absorption peak positions, but found instead able to eliminate residual aggregation present for the complex in both solvents and also to stop the tendency observed in DMF to undergo a one-electron reduction; such a type of problems was also encountered for the parent Zn^{II} pyrazinoporphyrazine complex $[(PdCl_2)_4Py_8TPyzPzZn]$.[3]

https://doi.org/10.1021/acs.inorgchem.1c01195
Inorg. Chem. XXXX, XXX, XXX−XXX

The two couples of complexes $[(PdCl_2)_4Py_8PzM]$ and $[\{Pd(CBT)_2\}_4Py_8PzM]$ (M = $Mg^{II}(H_2O)$ and Zn^{II}) show in DMSO and DMF (Figure 6; data in Table 1) narrow intense

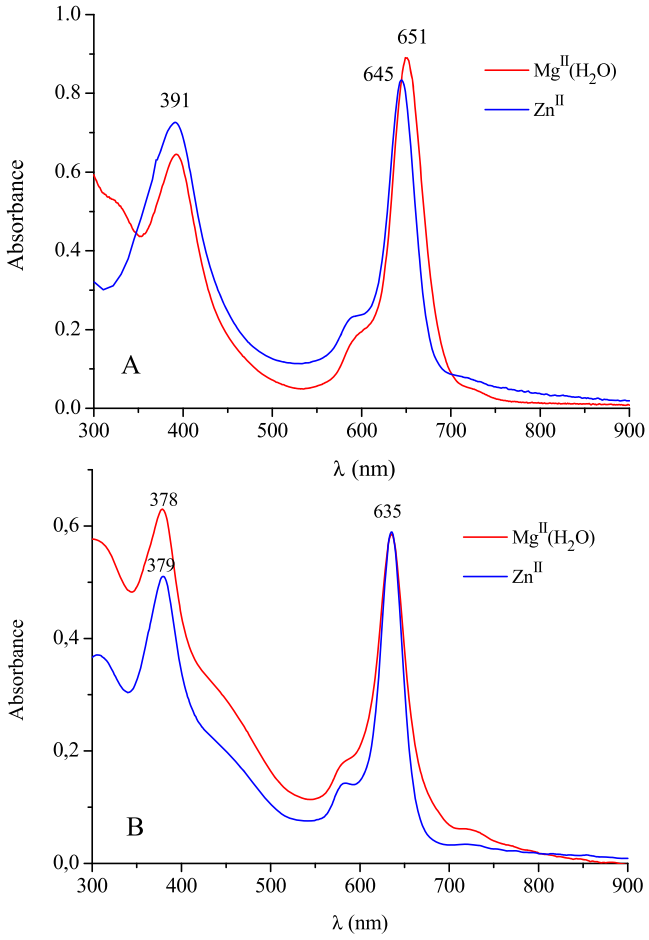

Figure 6. UV−visible spectra in DMSO solution of (A) $[(PdCl_2)_4Py_8PzM]$ and (B) $[\{Pd(CBT)_2\}_4Py_8PzM]$ (M = $Mg^{II}(H_2O)$, Zn^{II}).

absorptions in the Soret (350−400 nm) and Q-band region (600−650 nm), assigned as ligand-centered $\pi \rightarrow \pi^*$ transitions, positions of peaks indicative for both types of complexes of minimal/null solvent effects. Noteworthy, for both the CBT Mg^{II} and Zn^{II} complexes, an additional broad intense absorption is present in the range 400−500 nm (Figure 6B), absent not only for the analogues carrying externally $PdCl_2$ units (Figure 6A) but also in the spectra of the related mononuclear species $[Py_8PzM]$ (Table 1); these findings are the object of further discussion below.

Comparison of the spectral data of the complexes $[(PdCl_2)_4Py_8PzM]$ ($Mg^{II}(H_2O)$, Zn^{II}) with those of the homopentanuclear Pd^{II} analogue $[(PdCl_2)_4Py_8PzPd]$ (Table 1) indicates a dependence of the band positions on the type of central metal ion, as proved by the fact that the presence in the latter species of central Pd^{II} determines a remarkable hypsochromic shift of the Soret (40−45 nm) and Q-band positions (20−25 nm), shifts paralleling those observed also for the parent series of more extended macrocycles $[(PdCl_2)_4Py_8TPyzPzM]$ ($Mg^{II}(H_2O)$, Zn^{II}, Pd^{II}).[2c,3] This means that for homopentanuclear complex $[(PdCl_2)_4Py_8PzPd]$ and its analogue $[(PdCl_2)_4Py_8TPyzPzPd]$, a sensibly higher $\pi \rightarrow \pi^*$ transition energy occurs with respect to that of the related complexes carrying centrally $Mg(H_2O)$ and Zn^{II}. As a further UV−visible spectral notice, it has been observed that, owing to a moderate peripheral electron-withdrawing effect caused by the $PdCl_2$ external coordination in the pentanuclear species, as obtained from the corresponding mononuclear macrocycles $[Py_8PzM]$ (M = $Mg^{II}(H_2O)$, Zn^{II}, Pd^{II}; Table 1), a bathochromic shift of the Soret (5−10 nm) and Q-band positions (5−15 nm), meaning a reduction of the HOMO−LUMO gap, is also displayed; spectral changes here again recall those observed for the analogous $Mg(H_2O)$ and Zn^{II} tetrapyrazinoporphyrazines,[2c] minimal (in DMSO) for the Pd^{II} species.[3]

Noteworthy, data in Table 1 also inform that, differently from that observed for the macrocycles $[(PdCl_2)_4Py_8PzM]$ ($Mg^{II}(H_2O)$, Zn^{II}), practically no change is determined in the UV−visible peak positions when moving from the mononuclear $[Py_8PzM]$ to the corresponding CBT derivatives $[\{Pd(CBT)_2\}_4Py_8PzM]$. These data, recalling those observed for the parent tetrapyrazinoporphyrazines,[7] clarify that external coordination of the $Pd(CBT)_2$ moieties determines no relevant electronic perturbation in the central macrocyclic core.

As noted above, the presence of a broad absorption in the 400−500 nm region accompanying the Soret and Q bands in the UV−visible spectra run in DMSO (Figure 6B) and DMF solution for the two CBT macrocycles $[\{Pd(CBT)_2\}_4Py_8PzM]$ (M = $Mg^{II}(H_2O)$, Zn^{II}) is exclusive for them, since this absorption is not present in the spectra of the analogues $[(PdCl_2)_4Py_8PzM]$ (Figure 6A) from which the complexes are generated nor in the spectra of the respective mononuclear $[Py_8PzM]$ species (Table 1). Evidently, then, the occurrence of the 400−500 nm band for the CBT derivatives is strictly connected with the presence of such type of external moieties. It is also interesting to note that dissolution of both the Mg^{II} and Zn^{II} complexes in pyridine determines immediate releasing of the peripheral $Pd(CBT)_2$ fragments. The spectrum in fact, showing the complete absence of the 400−500 nm band, coincides perfectly with that expected for the mononuclear species $[Py_8PzM]$, the process taking place then being

$$[\{Pd(CBT)_2\}_4Py_8PzM] \rightarrow [Py_8PzM] + 4\ Pd(CBT)_2$$

a reaction also verified to occur for the pyrazinoporphyrazine analogues $[\{Pd(CBT)_2\}_4Py_8TPyzPzM]$.[7] Accordingly, it was observed that partial evaporation of the pyridine solution of the Zn^{II} macrocycle $[\{Pd(CBT)_2\}_4Py_8PzZn]$ allowed isolation of a solid material identified as the mononuclear species $[Py_8PzZn]$. Further evaporation of the solution determined isolation of the released $Pd(CBT)_2$ units in the form of the adduct $[py_2Pd(CBT)_2]$. From these results, it can be argued that the broad band at 400−500 nm observed for the intact pentanuclear macrocycles is intimately connected with the presence of the peripheral cis-arranged coordination sites "$py_2Pd(CBT)_2$" (py intended as the 2-pyridyl ring of the macrocycle) in them, a matter further supporting what previously pointed out for the analogous series of CBT tetrapyrazinoporphyrazines $[\{Pd(CBT)_2\}_4Py_8TPyzPzM]$.[7] On this point, a relevant aspect deserving mention is that the same absorption at 400−500 nm is also observed in the spectrum of the CBT derivative of formula *cis*-$[(bipy)Pd(CBT)_2]$ (bipy = 2,2′-bipyridyl) of structure elucidated by X-ray analysis.[20] Moreover, the absorption at 400−500 nm is not present in the UV−visible spectrum of the species *trans*-$[py_2Pd(CBT)_2]$, of known X-ray structure.[7] These data definitely support that the

https://doi.org/10.1021/acs.inorgchem.1c01195
Inorg. Chem. XXXX, XXX, XXX−XXX

Table 1. UV−Visible Spectral Data (λ, nm ($\log \varepsilon$)) of the Complexes $[(PdCl_2)_4Py_8PzM]$ and $[Py_8PzM]$ (M = $Mg^{II}(H_2O)$, Zn^{II}, Pd^{II}) and Those of Formula $[\{Pd(CBT)_2\}_4Py_8PzM]$ (M = $Mg^{II}(H_2O)$, Zn^{II}) in Different Solvents

		Soret region		Q-band region	
compound[a]	solvent	λ (nm)		(ε)	
$[(PdCl_2)_4Py_8PzMg(H_2O)]$	DMSO	391 (4.62)		589 (4.08)	651 (4.74)
	DMF	389 (4.60)		588 (4.15)	646 (4.63)
$[(PdCl_2)_4Py_8PzZn]$	DMSO[b]	391 (4.54)		588 (4.04)	645 (4.60)
	DMF[b]	396 (4.49)		587 (4.02)	643 (4.66)
$[(PdCl_2)_4Py_8PzPd]$[c]	DMSOl[b]	347		561	625
	DMF[b]	342		563	617
$[Py_8PzMg(H_2O)]$	DMSO	378 (4.52)		583 (3.95)	636 (4.63)
	DMF	378 (5.05)		583 (4.46)	636 (5.18)
$[Py_8PzZn]$	DMSO	380 (4.92)		584 (4.35)	636 (5.07)
	DMF	380 (4.82)		585 (4.26)	637 (4.98)
$[Py_8PzPd]$	DMSOl[b]	339 (4.42)		562 (3.95)	617 (4.44)
	DMFl[b]	339 (4.73)		557 (4.35)	612 (4.78)
$[\{Pd(CBT)_2\}_4Py_8PzMg(H_2O)]$	DMSO	378 (4.59)	452 (4.38)	579 (4.19)	635 (4.53)
	DMF	378 (4.87)	447 (4.59)	582 (4.34)	635 (4.84)
$[\{Pd(CBT)_2\}_4Py_8PzZn]$	DMSO	379 (4.86)	454 (4.44)	579 (4.33)	635 (4.92)
	DMF	379 (4.91)	448 (4.52)	580 (4.33)	635 (4.98)

[a]For all of the species, the data are referred to the corresponding hydrated formulas. [b]Solution in DMSO and DMF with HCl ($c = 2.0 \times 10^{-4}$ M). [c]Quantitative data could not be obtained due to the extensively present aggregation persistent also after addition of HCl.

presence of this absorption is intimately connected with the cis-arrangement of the $Pd(CBT)_2$ moiety, regardless of the substituents on the other two coordination positions. Conclusively then, these findings unequivocally call for a role in the macrocyclic species of the peripheral Pd^{II} coordination sites and their S functionalities, where they are present as *cis*-$N_2Pd(CBT)_2$ fragments.

Singlet Oxygen Quantum Yield Measurements on the Complexes $[(PdCl_2)_4Py_8PzM]$ and $[\{Pd(CBT)_2\}_4Py_8PzM]$ (M = $Mg^{II}(H_2O)$, Zn^{II}). The involvement of porphyrins and phthalocyanines[21] as photosensitizers for the generation of singlet oxygen ($^1O_2$) is of expanding interest for studies in the area of photodynamic therapy (PDT), whereas porphyrazines, in general, have so far received only limited attention, pertinent work having been mostly devoted to the photoactivity of seco-,[22] benzonaphtho-,[23] quinoxalino-,[24] and pyrazinoporphyrazines.[1b,2d,3−13,25] The efficiency of a macrocyclic photosensitizer depends on its tendency to undergo excitation upon irradiation from the ground state S_0 to the triplet state T1 with a high quantum yield, and also on having an adequate T1 energy and lifetime for a proper energy transfer to dioxygen for the process $^3O_2 \rightarrow {}^1O_2$ to occur. The type of metal center in the macrocycle can strongly influence this process, and, in this regard, it is known that closed-shell metal centers like Zn^{II} and Mg^{II} lead to high photoactivity, as do, in some cases, open-shell diamagnetic d^8 metal centers like Pd^{II} and Pt^{II}. In the present work, results are presented on the photosensitizing activity of $[(PdCl_2)_4Py_8PzM]$ and $[\{Pd(CBT)_2\}_4Py_8PzM]$ (M = $Mg^{II}(H_2O)$, Zn^{II}) for the generation of singlet oxygen, $^1O_2$. The quantum yields of singlet oxygen (Φ_Δ) (Table 2) were obtained in DMF and/or in a DMF/HCl mixture ([HCl] = 2×10^{-4} M) with a macrocycle concentration of ca. 10^{-6}−10^{-5} M. The procedure described in the Experimental Section is based on an absolute method, using a laser source at 650 nm close to the maximum of the Q-band absorption peaks of the complexes $[(PdCl_2)_4Py_8PzM]$ (M = $Mg^{II}(H_2O)$, Zn^{II}) and at 635 nm for the corresponding CBT derivatives $[\{Pd(CBT)_2\}_4Py_8PzM]$. Solutions of both series of porphyrazines were found stable under laser irradiation during the experiments. For the Zn^{II} complex $[(PdCl_2)_4Py_8PzZn]$, measurements of Φ_Δ were carried out in DMF/HCl because of the tendency of this species to undergo one-electron reduction processes in DMF at low concentrations (ca. 10^{-6}−10^{-5} M), similarly to that reported for the analogous pyrazinoporphyrazine Zn^{II} species $[(PdCl_2)_4Py_8TPyzPzZn]$.[3] The related Mg^{II} complex $[(PdCl_2)_4Py_8PzMg(H_2O)]$ was examined in pure DMF since the addition of HCl to solution led to spectral changes, one reason for that presumably residing on the slow releasing of the central Mg^{II} and formation of the unknown corresponding centrally unmetalated species (M = $2H^I$). The same reason is hypothetically valid also for the CBT/Mg^{II} analogue for which the spectral changes were also observed in the presence of HCl.

Table 2. Singlet Oxygen Quantum Yields (Φ_Δ) in DMF and/or DMF/HCl of $[\{Pd(CBT)_2\}_4Py_8PzM]$, $[(PdCl_2)_4Py_8PzM]$ and Related Pyrazinoporpyrazines; M = $Mg^{II}(H_2O)$, Zn^{II}

compound	λ_{max} [nm]	λ_{irr} [nm]	Φ_Δ[a]	ref
$[(PdCl_2)_4Py_8PzMg(H_2O)]$	648	650	0.34	this work
$[(PdCl_2)_4Py_8PzZn]$	644	650[b]	0.52	this work
$[\{Pd(CBT)_2\}_4Py_8PzMg(H_2O)]$	634	635	0.29	this work
$[\{Pd(CBT)_2\}_4Py_8PzZn]$	635	635	0.55	this work
$[(PdCl_2)_4Py_8TPyzPzMg(H_2O)]$	662	670	0.23	7
$[(PdCl_2)_4Py_8TPyzPzZn]$	662	670[c]	0.48	7
$[\{Pd(CBT)_2\}_4Py_8TPyzPzMg(H_2O)]$	658	650	0.25	7
$[\{Pd(CBT)_2\}_4Py_8TPyzPzZn]$	656	650	0.65	7

[a]Mean value of at least three measurements. Uncertainty is half-dispersion, and it is typically ±0.03. [b]DMF preacidified with HCl 2.0×10^{-4} M. [c]DMF preacidified with HCl $1.0 \times 10-^4$ M.

Figure 7 shows the UV−visible spectral data and the relative Stern−Volmer analysis (eq 1) obtained in a typical experiment

https://doi.org/10.1021/acs.inorgchem.1c01195
Inorg. Chem. XXXX, XXX, XXX−XXX

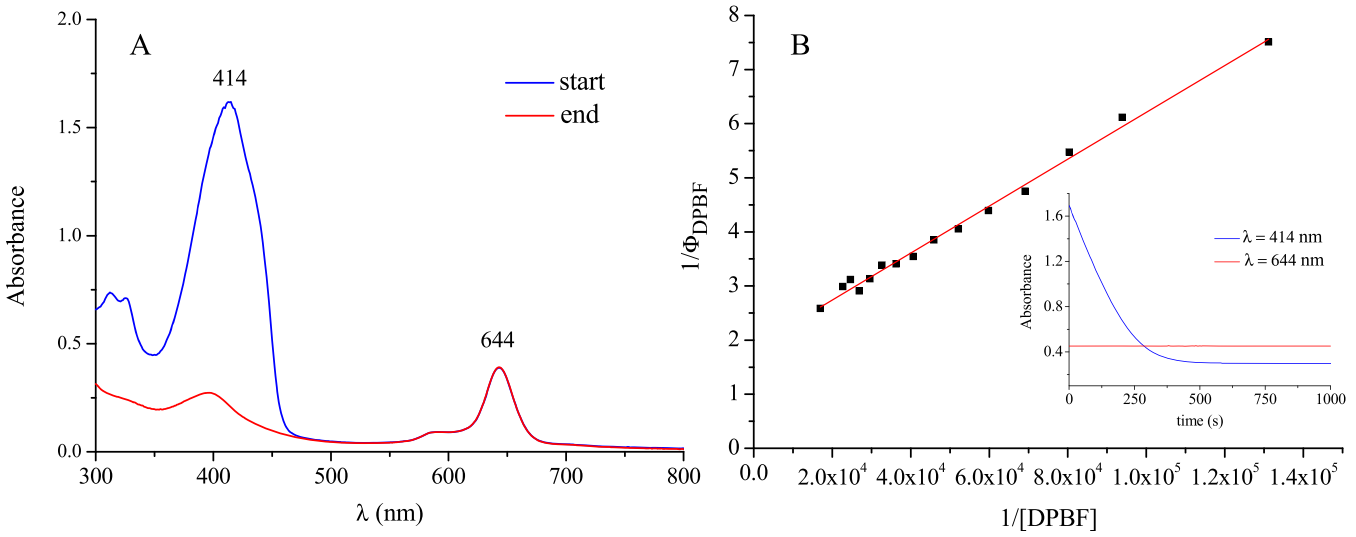

Figure 7. (A) UV−visible spectra in DMF solution of $[(PdCl_2)_4Py_8PzZn]$ and DPBF before (blue line) and after (red line) laser irradiation (λ_{irr} = 650 nm). (B) Stern−Volmer data analysis of the DPBF photooxidation (DPBF absorption decay at 414 nm is shown in the inset; the red dotted line indicates the stability of the complex during irradiation).

carried out with the Zn^{II} derivative $[(PdCl_2)_4Py_8PzZn]$ and used to calculate the singlet oxygen quantum yield value (Φ_Δ) of the complex. Figure 7 and the inset of Figure 7B illustrate the absorption decay recorded at 414 nm for the $^1O_2$ scavenger, DPBF, during irradiation and as well the stability of the complex under the utilized experimental conditions. As evident from Table 2, the measured Φ_Δ values follow the order $Zn^{II} > Mg^{II}$. This is in agreement with the "heavy atom effect", which enhances the triplet excited state quantum yield for Zn^{II} with respect to Mg^{II}. Indeed, the introduction of a heavier metal ion into a porphyrazine macrocycle increases the rate of intersystem crossing via enhancement of spin−orbit coupling, thus favoring the formation of a triplet state T1 with adequate energy and lifetime to allow a proper energy transfer to dioxygen for the process $^3O_2 \rightarrow {}^1O_2$. The Φ_Δ values of the Zn^{II} complexes $[(PdCl_2)_4Py_8PzZn]$ (0.52) and $[\{Pd(CBT)_2\}_4Py_8PzZn]$ (0.55) in DMF fall in the range of 0.4−0.6 previously reported for a number of Zn^{II} phthalocyanines and porphyrazines,[25−28] including porphyrazine macrocycles studied by our group.[2d,3,7,13,29] The overall results qualify these compounds as highly efficient photosensitizers for the generation of singlet oxygen and, with regard to the CBT derivatives, as promising species for potential applications in PDT/BNCT combined therapies.

CONCLUSIONS

In previous and more recent research work, all our attempts failed in the direct synthesis of the porphyrazine macrocycle octakis(2-pyridyl)porphyrazine, $[Py_8PzH_2]$, by automacrocyclization of the potential precursor 1,2-dicyano-1,2-di(2-pyridyl)-ethylene, $[(CN)_2Py_2Et]$, against the successful process instead obtained for the more expanded macrocyclic analogue tetrakis-2,3-[5,6-di(2-pyridyl)-pyrazino]porphyrazine, $[Py_8TPyzPzH_2]$, using as a precursor 2,3-dicyano-5,6-di(2-pyridyl)-1,4-pyrazine, $[(CN)_2dpp]$.[30] The macrocyclization process of $[(CN)_2Py_2Et]$ could be operated in the presence of metallic Mg with the formation of the Mg^{II} porphyrazine species $[Py_8PzMg(H_2O)]$, the basic material which could lead to the here reported and studied pentanuclear porphyrazine macrocycles $[(PdCl_2)_4Py_8PzM]$ (M = $Mg^{II}(H_2O)$, Zn^{II}, Pd^{II})) (implied transmetalation processes cited in the text for $[Py_8PzZn]$ and $[(PdCl_2)_4Py_8PzPd]$) and $[\{Pd(CBT)_2\}_4Py_8PzM]$ (M = $Mg^{II}(H_2O)$, Zn^{II}), and the mononuclear Pd^{II} complex $[Py_8PzPd]$, all of the species obtained in a hydrated form. The examination of IR spectra provides useful information about correct formulation and purity for each species evidencing also specific absorptions for the external $PdCl_2$ and CBT units in the respective macrocycles. The UV−visible spectra in the DMSO and DMF solution of both series of pentanuclear complexes is generally indicative of the absence of significant aggregation and characterized by the expected intense Soret (300−400 nm) and Q bands (600−700 nm) with peak positions depending on the type of central metal and external units ($PdCl_2$; CBT substituents). Characteristic for the two CBT derivatives is the presence of a broad band in the region 400−500 nm certainly attributable to the type of direct contacts occurring between the CBT groups (through their S atoms) and the Pd^{II} internal sorroundings. Detachment in pyridine solution of the external $Pd(CBT)_2$ units determines the formation of the mononuclear core $[Py_8PzM]$ (M = $Mg^{II}(H_2O)$, Zn^{II}) and isolation of the compound *trans*-$[py_2Pd(CBT)_2]$ already known since isolated previously in the parallel detachment operated for the more expanded macrocycles $[\{Pd(CBT)_2\}_4Py_8PzM]$ (M = $Mg^{II}(H_2O)$, Zn^{II}). A high level of singlet oxygen quantum yield values for the two Zn^{II} species (Table 1, Φ_Δ = 0.52−0.55), with respect to the rule since presenting $\Phi_{\Delta(ZnII)} > \Phi_{\Delta(MgII)}$, is promising in terms of potential PDT response and positive bimodal activity PDT/BNCT expected as possible for the CBT derivatives.

AUTHOR INFORMATION

Corresponding Author

Maria Pia Donzello − *Dipartimento di Chimica, Università degli Studi di Roma Sapienza, I-00185 Rome, Italy;* orcid.org/0000-0001-9084-0369; Email: maiapia.donzello@uniroma1.it

Authors

Noemi Bellucci − *Dipartimento di Chimica, Università degli Studi di Roma Sapienza, I-00185 Rome, Italy*

https://doi.org/10.1021/acs.inorgchem.1c01195
Inorg. Chem. XXXX, XXX, XXX−XXX

Elisa Viola − *Dipartimento di Chimica, Università degli Studi di Roma Sapienza, I-00185 Rome, Italy*
Claudio Ercolani − *Dipartimento di Chimica, Università degli Studi di Roma Sapienza, I-00185 Rome, Italy*

Complete contact information is available at:
https://pubs.acs.org/10.1021/acs.inorgchem.1c01195

Notes

The authors declare no competing financial interest.

■ ACKNOWLEDGMENTS

Financial support by the University of Rome Sapienza (Progetto di Ricerca—Anno 2019-RP11916B889D3C2D) is gratefully acknowledged. M.P.D. is grateful to the Consorzio Interuniversitario di Ricerca in Chimica dei Metalli nei Sistemi Biologici (CIRCMSB) for scientific support. Prof. Alessia Ciogli is gratefully acknowledged for the MS-ESI measurements.

■ REFERENCES

(1) (a) Donzello, M. P.; Ercolani, C.; Novakova, V.; Zimcik, P.; Stuzhin, P. A. Tetrapyrazinoporphyrazines and Their Metal Derivatives. Part I: Synthesis and Basic Structural Information. *Coord. Chem. Rev.* **2016**, *309*, 107−179. (b) Novakova, V.; Donzello, M. P.; Ercolani, C.; Zimcik, P.; Stuzhin, P. Tetrapyrazinoporphyrazines and Their Metal Derivatives. Part II: Electronic Structure, Electrochemical, Spectral, Photophysical and Other Application Related Properties. *Coord. Chem. Rev.* **2018**, *361*, 1−73.

(2) (a) Donzello, M. P.; Ou, Z.; Dini, D.; Meneghetti, M.; Ercolani, C.; Kadish, K. M. Tetra-2,3-pyrazinoporphyrazines with Externally Appended Pyridine Rings. 2. Metal Complexes of Tetrakis-2,3-[5,6-di(2-pyridyl)pyrazino]porphyrazine: Linear and Nonlinear Optical Properties and Electrochemical Behavior. *Inorg. Chem.* **2004**, *43*, 8637−8648. (b) Bergami, C.; Donzello, M. P.; Monacelli, F.; Ercolani, C.; Kadish, K. M. Tetra-2,3-pyrazinoporphyrazines with Externally Appended Pyridine Rings. 4. UV−Visible Spectral and Electrochemical Evidence of the Remarkable Electron-Deficient Properties of the New Tetrakis-2,3-[5,6-di{2-(N-methyl)-pyridiniumyl}pyra-zino]porphyrazinatometal Octacations, $[(2\text{-Me-py})_8\text{TPyzPzM}]^{8+}$ (M = $Mg^{II}(H_2O)$, Co^{II}, Cu^{II}, Zn^{II}). *Inorg. Chem.* **2005**, *44*, 9862−9873. (c) Donzello, M. P.; Viola, E.; Cai, X.; Mannina, L.; Rizzoli, C.; Ricciardi, G.; Ercolani, C.; Kadish, K. M.; Rosa, A. Tetra-2,3-pyrazinoporphyrazines with Externally Appended Pyridine Rings. 5. Synthesis, Physicochemical and Theoretical Studies of a Novel Pentanuclear Palladium(II) Complex and Related Mononuclear Species. *Inorg. Chem.* **2008**, *47*, 3903−3919. (d) Donzello, M. P.; Viola, E.; Mannina, L.; Barteri, M.; Fu, Z.; Ercolani, C. Tetra-2,3-pyrazinoporphyrazines with externally appended pyridine rings. 11. Photoactivity of a new Pt(II) pentanuclear macrocycle bearing four cisplatin-like functionalities and its related monoplatinated species. *J. Porphyrins Phthalocyanines* **2011**, *15*, 984−994.

(3) Donzello, M. P.; Viola, E.; Cai, X.; Mannina, L.; Ercolani, C.; Kadish, K. M. Tetra-2,3-pyrazinoporphyrazines with Externally Appended Pyridine Rings. 8. Central (Zn^{II}, Cu^{II}, $Mg^{II}(H_2O)$, Cd^{II}) and Exocyclic (PdII) Metal Ion Binding in Heteropentametallic Complexes from Tetrakis-2,3-[5,6-di(2-pyridyl)pyrazino]-porphyrazine. *Inorg. Chem.* **2010**, *49*, 2447−2456.

(4) (a) Donzello, M. P.; Vittori, D.; Viola, E.; Manet, I.; Mannina, L.; Cellai, L.; Monti, S.; Ercolani, C. Tetra-2,3-pyrazinoporphyrazines with Externally Appended Pyridine Rings. 9. Novel Heterobimetallic Macrocycles and Related Hydrosoluble Hexacations as Potentially Active Photo/Chemotherapeutic Anticancer Agents. *Inorg. Chem.* **2011**, *50*, 7391−7402. (b) Donzello, M. P.; Vittori, D.; Futur, D.; Fu, Z.; Ercolania, C.; Kadish, K. M. Tetra-2,3-pyrazinoporphyrazines with externally appended pyridine rings. 14. UV−visible spectral and electrochemical behavior of homo/heterobinuclear neutral and hexacationic macrocycles. *J. Porphyrins Phthalocyanines* **2013**, *17*, 896−904.

(5) (a) Donzello, M. P.; Vittori, D.; Viola, E.; Zeng, L.; Cui, Y.; Kadish, K. M.; Mannina, L.; Ercolani, C. Tetra-2,3-pyrazinoporphyrazines with externally appended pyridine rings. 16. A rare class of uncharged water soluble complexes: UV−vis spectral, redox, and photochemical properties. *J. Porphyrins Phthalocyanines* **2015**, *19*, 903−919. (b) Viola, E.; Donzello, M. P.; Sciscione, F.; Shah, K.; Ercolani, C.; Trigiante, G. Tetra-2,3-pyrazinoporphyrazines with externally appended pyridine rings. 17. Photosensitizing properties and cellular effects of Zn^{II} octacationic and Zn^{II}/Pt^{II} hexacationic macrocycles in aqueous media: Perspectives of multimodal anticancer potentialities. *J. Photochem. Photobiol. B* **2017**, *169*, 101−109.

(6) Manet, I.; Manoli, F.; Donzello, M. P.; Viola, E.; Andreano, G.; Masi, A.; Cellai, L.; Monti, S. A cationic Zn^{II} porphyrazine induces a stable parallel G-quadruplex conformation in human telomeric DNA. *Org. Biomol. Chem.* **2011**, *9*, 684−688.

(7) Viola, E.; Donzello, M. P.; Testani, S.; Luccisano, G.; Astolfi, M. L.; Rizzoli, C.; Cong, L.; Mannina, L.; Ercolani, C.; Kadish, K. M. Tetra-2,3-pyrazinoporphyrazines with Peripherally Appended Pyridine Rings. 19. Pentanuclear Octa(2-pyridyl)-tetrapyrazinoporphyrazines Carrying Externally Carboranthiolate Groups: Physicochemical Properties and Potentialities as Anticancer Drugs. *Inorg. Chem.* **2019**, *58*, 1120−1133.

(8) Kharasch, M. S.; Seyler, R. C.; Mayo, F. R. Coordination Compounds of Palladous Chlorid. *J. Am. Chem. Soc.* **1938**, *60*, 882−884.

(9) Donzello, M. P.; De Mori, G.; Viola, E.; Ercolani, C.; Ricciardi, G.; Rosa, A. Tetra-2,3-pyrazinoporphyrazines with Externally Appended Pyridine Rings. 15. Effects of the Pyridyl Substituents and Fused Exocyclic Rings on the UV−Visible Spectroscopic Properties of Mg(II)- Porphyrazines: A Combined Experimental and DFT/TDDFT Study. *Inorg. Chem.* **2014**, *53*, 8009−8019.

(10) Sciscione, F.; Cong, L.; Donzello, M. P.; Viola, E.; Ercolani, C.; Kadish, K. M. Octakis(2-pyridyl)porphyrazine and Its Neutral Metal Derivatives: UV-Visible Spectral, Electrochemical, and Photoactivity Studies. *Inorg. Chem.* **2017**, *56*, 5813−5826.

(11) Donzello, M. P.; Viola, E.; Giustini, M.; Ercolani, C.; Monacelli, F. Tetrakis(thiadiazole)porphyrazines. 8. Singlet oxygen production, fluorescence response and liposomal incorporation of tetrakis-(thiadiazole) porphyrazine macrocycles [TTDPzM] (M = $Mg^{II}(H_2O)$, Zn^{II}, $Al^{III}Cl$, $Ga^{III}Cl$, Cd^{II}, Cu^{II}, $2H^{I}$). *Dalton Trans.* **2012**, *41*, 6112−6121.

(12) Viola, E.; Donzello, M. P.; Ciattini, S.; Portalone, G.; Ercolani, C. Redox Chemistry of Tetrakis[5,6-di(2-pyridyl)-2,3-pyrazino]-porphyrazinatocobalt(II): Isolation and Characterization of Solid Pure Co^{I}, Co^{II}, and Co^{III} Complexes. *Eur. J. Inorg. Chem.* **2009**, *2009*, 1600−1607.

(13) Donzello, M. P.; Viola, E.; Ercolani, C.; Fu, Z.; Futur, D.; Kadish, K. M. Tetra-2,3-pyrazinoporphyrazines with Externally Appended Pyridine Rings. 12. New Heteropentanuclear Complexes Carrying Four Exocyclic Cis-platin-like Functionalities as Potential Bimodal (PDT/Cis-platin) Anticancer Agents. *Inorg. Chem.* **2012**, *51*, 12548−12559.

(14) Velazquez, C. S.; Fox, G. A.; Broderick, W. E.; Andersen, K. A.; Anderson, O. P.; Barret, A. G. M.; Hoffman, B. M. star-Porphyrazines: synthetic, structural, and spectral investigation of complexes of the polynucleating porphyrazine octathiolato ligand. *J. Am. Chem. Soc.* **1992**, *114*, 7416−7424.

(15) Templeton, D. H.; Fischer, M. S.; Zalkin, A.; Calvin, M. Structure and chemistry of theporphyrins. Crystal and molecular structure of the monohydrated dipyridinated magnesium phthalocyanine complex. *J. Am. Chem. Soc.* **1971**, *93*, 2622−2628.

(16) Donzello, M. P.; Stuzhin, P. A.; Ercolani, C. Novel families of phthalocyanine-like macrocycles-Porphyrazines with annulated strongly electron-withdrawing 1,2,5-thia/selenodiazole rings. *Coord. Chem. Rev.* **2006**, *250*, 1530−1561.

(17) Matzumoto, S.; Endo, A.; Mizuguchi, J. Structure of magnesium phthalocyanine complexes. *Z. Krystallogr.* **2000**, *215*, 182−186.

https://doi.org/10.1021/acs.inorgchem.1c01195
Inorg. Chem. XXXX, XXX, XXX−XXX

(18) Baum, S. M.; Trabanco, A. A.; Montalban, A. G.; Micallef, A. S.; Zhong, C.; Meunier, H. G.; Suhling, K.; Phillips, D.; White, A. J. P.; Williams, D. J.; Barrett, A. G. M.; Hoffman, B. M. Synthesis and Reactions of Aminoporphyrazines with Annulated Five- and Seven-Membered Rings. *J. Org. Chem.* **2003**, *68*, 1665−1670.

(19) Leites, L. A. Vibrational spectroscopy of carboranes and parent boranes and its capabilities in carborane chemistry. *Chem. Rev.* **1992**, *92*, 279−323.

(20) X-ray structure and related UV−visible spectra reported in manuscript submitted to the Inorganic Chemistry Journal.

(21) (a) O'Connor, A. E.; Gallagher, W. M.; Byrne, A. T. Porphyrin and Nonporphyrin Photosensitizers in Oncology: Preclinical and Clinical Advances in Photodynamic Therapy. *Photochem. Photobiol.* **2009**, *85*, 1053−1074. (b) Szaciłowski, K.; Macyk, W.; Drzewiecka-Matuszek, A.; Brindell, M.; Stochel, G. *Chem. Rev.* **2005**, *105*, 2647−2694. (c) Lukyanets, E. A. Phthalocyanines as photosensitizers in the photodynamic therapy of cancer. *J. Porphyrins Phthalocyanines* **1999**, *3*, 424−432. (d) Sekkat, N.; van den Bergh, H.; Nyokong, T.; Lange, N. Like a bolt from the blue: Phthalocyanines in biomedical optics. *Molecules* **2012**, *17*, 98−144.

(22) (a) Sakellariou, E. G.; Montalban, A. G.; Meunier, H.; Rumbles, G.; Philips, D.; Ostier, R. B.; Suhling, K.; Barrett, A. G. M.; Hoffman, B. M. Peripherally Metalated Secoporphyrazines: A New Generation of Photoactive Pigments. *Inorg. Chem.* **2002**, *41*, 2182−2187. (b) Montalban, A. G.; Baum, S. M.; Barrett, A. G. M.; Hoffman, B. M. Studies on seco-porphyrazines: a case study on serendipity. *Dalton Trans.* **2003**, *40*, 2093−2102.

(23) Michelsen, U.; Kliesch, H.; Schnurpfeil, G.; Sobbi, A. K.; Wöhrle, D. Un symmetrica My Substituted Benzonaphthoporphyrazines: A New Class of Cationic Photosensitizers for the Photodynamic Therapy of Cancer. *Photochem. Photobiol.* **1996**, *64*, 694−701.

(24) Mitzel, F.; FitzGerald, S.; Beeby, A.; Faust, R. Acetylenic Quinoxalinoporphyrazines as Photosensitizers for Photodynamic Therapy. *Chem. − Eur. J.* **2003**, *9*, 1233−1241.

(25) (a) Novakova, V.; Morkved, E. H.; Miletin, M.; Zimcik, P. Influence of protonation of peripheral substituents on photophysical and photochemical properties of tetrapyrazinoporphyrazines. *J. Porphyrins Phthalocyanines* **2010**, *14*, 582−591. (b) Zimcik, P.; Novakova, V.; Miletin, M.; Kopecky, K. Thianaphthene-Annulated Tetrapyrazinoporphyrazines. *Macroheterocycles* **2008**, *1*, 21−29. (c) Zimcik, P.; Miletin, M.; Novakova, V.; Kopecky, K.; Nejedla, M.; Stara, V.; Sedlackova, K. Effective Monofunctional Azaphthalocyanine Photosensitizers for Photodynamic Therapy. *Aust. J. Chem.* **2009**, *62*, 425−433. (d) Mitzel, F.; Fitzgerald, S.; Beeby, A.; Faust, R. The Synthesis of Arylalkyne-Substituted Tetrapyrazinoporphyrazines and an Evaluation of Their Potential as Photosensitisers for Photodynamic Therapy. *Eur. J. Org. Chem.* **2004**, *2004*, 1136−1142. (e) Machacek, M.; Cidlina, A.; Novakova, V.; Svec, J.; Rudolf, E.; Miletin, M.; Kučera, R.; Simunek, T.; Zimcik, P. Far-Red-Absorbing Cationic Phthalocyanine Photosensitizers: Synthesis and Evaluation of the Photodynamic Anticancer Activity and the Mode of Cell Death Induction. *J. Med. Chem.* **2015**, *58*, 1736−1749.

(26) (a) Kushwah, N. P.; Jain, V. K.; Wadawale, A.; Zhidkova, O. B.; Starikova, Z. A.; Bregadze, V. I. Synthesis, spectroscopy and structures of palladium(II) and platinum(II) complexes containing mercapto-o-carborane. *J. Organomet. Chem.* **2009**, *694*, 4146−4151. (b) Teixidor, F.; Laromaine, A.; Kivekas, R.; Sillanpaa, R.; Vinas, C.; Vespalec, R.; Horakova, H. Synthesis, reactivity and complexation studies of N,S exo-heterodisubstituted o-carborane ligands. Carborane as a platform to produce the uncommon bidentate chelating (pyridine)N-C-C-C-S(H) motif. *Dalton Trans.* **2008**, 345−354. (c) Crujeiras, P.; Rodriguez-Rey, J. L.; Sousa-Pedrares, A. Deactivation of the coordinating ability of the iminophosphorane group by the effect of ortho-carborane. *Dalton Trans.* **2017**, 2572−2593. (d) Kennedy, R. D.; Stern, C. L.; Mirkin, C. A. Zwitterionic Weak-Link Approach Complexes Based on Anionic Icosahedral Monocarbaboranes. *Inorg. Chem.* **2013**, *52*, 14064−14071.

(27) Wöhrle, D.; Tsaryova, O.; Semioshkin, A.; Gabel, D.; Suvorova, O. Synthesis and photochemical properties of phthalocyanine zinc(II) complexes containing o-carborane units. *J. Organomet. Chem.* **2013**, *747*, 98−105.

(28) Nyokong, T. Effects of substituents on the photochemical and photophysical properties of main group metal phthalocyanines. *Coord. Chem. Rev.* **2007**, *251*, 1707−1722.

(29) Pietrangeli, D.; Rosa, A.; Pepe, A.; Altieri, S.; Bortolussi, S.; Postuma, I.; Protti, N.; Ferrari, C.; Cansolino, L.; Clerici, A. M.; Viola, E.; Donzello, M. P.; Ricciardi, G. Water-soluble carboranyl-phthalocyanines for BNCT. Synthesis, characterization, and in vitro tests of the Zn(II)-nido-carboranylhexylthiophthalocyanine. *Dalton Trans.* **2015**, *44*, 11021−11028.

(30) Donzello, M. P.; Ou, Z.; Monacelli, F.; Ricciardi, G.; Rizzoli, C.; Ercolani, C.; Kadish, K. M. Tetra-2,3-pyrazinoporphyrazines with Externally Appended Pyridine Rings. 1. Tetrakis-2,3-[5,6-di(2-pyridyl)pyrazino]porphyrazine: A New Macrocycle with Remarkable Electron-Deficient Properties. *Inorg. Chem.* **2004**, *43*, 8626−8636.

https://doi.org/10.1021/acs.inorgchem.1c01195
Inorg. Chem. XXXX, XXX, XXX−XXX